THE JOURNAL OF BIOLOGICAL CHEMISTRY
Vol. 263, No. 33, Issue of November 25, pp. 17566-17575, 1988
Printed in U.S.A.

Studies on the Electron Transfer Pathway, Topography of Iron-Sulfur Centers, and Site of Coupling in NADH-Q Oxidoreductase*

(Received for publication, October 26, 1987)

G. Krishnamoorthy‡ and Peter C. Hinkle

From the Section of Biochemistry, Molecular and Cell Biology, Division of Biological Sciences, Wing Hall, Cornell University, Ithaca, New York 14853

Electron transfer activities and steady state reduction levels of Fe-S centers of NADH-Q oxidoreductase were measured in mitochondria, submitochondrial particles (ETP_H), and complex I after treatment with various reagents. *p*-Chloromercuribenzenesulfonate destroyed the signal from center N-4 (g_x = 1.88) in ETP_H but not in mitochondria, showing that N-4 is accessible only from the matrix side of the inner membrane. *N*-Bromosuccinimide also destroyed the signal from N-4 but without inhibiting rotenone-sensitive electron transfer to quinone, suggesting a branched pathway for electron transfer. Diethylpyrocarbonate caused oxidation of N-3 and N-4 in the steady state without changing N-1, suggesting N-1 is before N-3 and N-4. Difluorodinitrobenzene and dicyclohexylcarbodiimide inhibited oxidation of all Fe-S centers and tetranitromethane inhibited reduction of all Fe-S centers.

Titrations of the rate of superoxide (O_2^-) generation in rotenone-treated submitochondrial particles were similar with the ratio [NADH]/[NAD] and that of 3-acetyl pyridine adenine nucleotide in spite of different midpoint potentials of the two couples. On reaction with inhibitors the inhibition of O_2^- formation was similar to that of ferricyanide reductase rather than quinone reductase. The rate of O_2^- formation during ATP-driven reverse electron transfer was 16% of the rate observed with NADH. The presence of NAD increased the rate to 83%. The results suggest that bound, reduced nucleotide, probably E-NAD*, is the main source of O_2^- in NADH dehydrogenase.

The effect of ATP on the reduction levels of Fe-S centers in well-coupled ETP_H was measured by equilibrating with either NADH/NAD or succinate/fumarate redox couples. With NADH/NAD none of the Fe-S centers showed ATP induced changes, but with succinate/fumarate all centers showed ATP-driven reduction with or without NAD present. The effect on N-2 was smaller than that on N-1, N-3, and N-4. These observations indicate that the major coupling interaction is between N-2 and the low potential centers, N-1, N-3, and N-4. Possible schemes of coupling in this segment are discussed.

NADH-Q oxidoreductase of the mitochondrial respiratory chain contains FMN and four or five Fe-S centers (for reviews see 1-5), but the path of electron transfer through these components and the site and mechanism of energy coupling are not well characterized. Potentiometric titrations combined with EPR (electron paramagnetic resonance) at low temperatures have revealed a major potential gap of about 300 mV between the Fe-S center N-2 ($E_{m,7} \sim -30$ mV) and the other Fe-S centers N-1, N-3, and N-4 ($E_{m,7} \sim -360$ to -260 mV) (2, 6). FMN has not been characterized due to spectral overlap of Fe-S chromophores. A variety of electron acceptors other than ubiquinone have been used. Electron transfer to ubiquinone analogs such as Q_1[1], duroquinone, and DB[1] quinone are rotenone sensitive whereas electron transfer to ferricyanide, juglone (5-hydroxy-1,4-naphthoquinone), 2,6-dichlorophenolindophenol, etc. are rotenone insensitive, showing different sites of electron donation from the complex. Rapid mixing and freezing techniques failed to resolve the electron transfer pathway from NADH due to fast intramolecular electron transfer (7, 8). Studies with sulfhydryl (for review, see 9) and other (10) reagents have shown several inhibition sites characterized by selective inhibition with different acceptors. The topographical organization of the constituent polypeptides was studied by labeling with hydrophilic and hydrophobic reagents (1, 11) and chemical cross-linking (12, 13). Also, the enzyme has been resolved into smaller fragments (14, 15). However such studies have been hampered by the lack of assignment of the fragments with the Fe-S centers which showed drastic changes in their EPR spectra on resolution (14, 15). Despite the complexity of this enzyme, the amino acid sequences of several subunits of complex I are now known from the mammalian mitochondrial genome (16).

NADH-Q oxidoreductase translocates H^+ coupled to the reduction of ubiquinone by NADH (17, 18). The effect of ATP energization on the apparent midpoint potentials of the Fe-S centers has been studied in order to evaluate their participation in energy coupling (2, 6, 19, 20). However, the results of these studies are quite contradictory. The stoichiometry at this site is at least 3-5 $H^+/2e^-$ (21-25). This cannot be explained by the classical loop mechanism (17) and more complex schemes (26) must be considered.

In this work, we have used inhibitors and chemical modifications on complex I, ETP_H, and intact mitochondria using a variety of reagents. We have measured the electron transfer rates to acceptors such as DB, ferricyanide, and O_2 and reduction levels of Fe-S centers either during steady-state

* This research was supported by National Institutes of Health Grant HL14483. The costs of publication of this article were defrayed in part by the payment of page charges. This article must therefore be hereby marked "*advertisement*" in accordance with 18 U.S.C. Section 1734 solely to indicate this fact.

‡ Present address: Chemical Physics Group, Tata Institute of Fundamental Research, Homi Bhabha Rd, Bombay 400 005, India.

[1] The abbreviations used are: DB, 2,3-methoxy-5-methyl-6-decyl-1,4-benzoquinone; Q, coenzyme Q_{10}; ETP_H, phosphorylating electron transport particles prepared from bovine heart mitochondria; PCMBS, *p*-chloromercuribenzenesulfonic acid; MOPS, 3-(*N*-morpholino)propanesulfonic acid; MES, 2-(*N*-morpholino)ethanesulfonic acid; NBS, *n*-bromosuccinimide; APADH, 3-acetyl pyridine adenine dinucleotide, reduced form.

(uncoupled) electron flow or in the energy-coupled state. We have correlated these results in terms of pathway of electron flow and mechanism of energy coupling.

MATERIALS AND METHODS

Complex I (27) and ETP_H (28) were prepared as described, except that Mn^{2+} was replaced by Mg^{2+}. Beef heart mitochondria (prepared on a small scale) (29) showed respiratory control ratios of 6 with pyruvate plus malate as substrates. Their NADH oxidase activity was about 10% of the activity of ETP_H showing that about 90% of the mitochondria were intact.

The reagents, except DCCD, used for chemical modification were obtained from Sigma. DCCD was obtained from Schwarz Mann. Myxothiazol was a generous gift from Dr. W. Trowitzsch (Gesellschaft für Biotechnologische Forschung, Braunschweig). The ubiquinone analog, DB (30) was a gift from Dr. Bernard Trumpower (Dartmouth Medical School). Tinopal AN was from Dr. A. M. Paton (University of Aberdeen).

Chemical modifications were generally carried out by the addition of the reagent to a suspension of complex I, ETP_H, or mitochondria (final protein concentration 1 mg ml^{-1}) in 250 mM sucrose, 10 mM K-MOPS, pH 7.5, and incubation at 25 °C for 30 min. In the case of PCMBS, the pH of the medium was varied from pH 6 to 9 using MES, MOPS, or Tris buffers. For studies on the sidedness of center N-4, the reaction with PCMBS was carried out at 4 °C (and pH 6.5) for 30 min in order to minimize the permeation of PCMBS into mitochondria. In the case of complex I, the reaction medium also contained sonicated soybean lipid to a final concentration of 2.5 mg ml^{-1}. The excess reagents were removed by pelleting the suspension at 100,000 × *g* and resuspending the pellet in 250 mM sucrose, 10 mM K-MOPS, pH 7.5, buffer to a final concentration of 20 to 40 mg of protein ml^{-1} concentrations, suitable for EPR measurements.

Samples for EPR measurements were prepared as follows. For measurements of steady state reduction levels of the Fe-S centers, the samples, treated as described in the previous paragraph, were treated with myxothiazol (except with complex I, final concentration 20 μg ml^{-1}) and DB (2 mM) and transferred into EPR tubes at 25 °C. NADH was added to a final concentration of 2 mM, and the sample was stirred for 2 to 4 s and then quickly frozen in a methylcyclohexane-isopentane (1:5) mixture cooled by liquid nitrogen. The oxidation of NADH (2 mM) in unmodified samples took about 15 s for completion as observed in a separate experiment. Myxothiazole and DB were dissolved in Me_2SO. Complete reduction of the Fe-S centers was achieved by reducing the sample by NADH and solid dithionite in the presence of 17 μM each of phenosafranine, methyl viologen, and benzyl viologen. Preparation of EPR samples for studies of the effect of ATP on the Fe-S centers in ETP_H is described in the legend to Table II.

EPR spectra were obtained using a Varian E-12 spectrometer operating at 9.2 GHz. Typical spectra are shown in Fig. 1*A*. The temperature of the sample was controlled by an Oxford Instrument Co. continuous flow helium cryostat. Quantitation of reduction levels of the Fe-S centers was done as follows (2, 3). N-1 was estimated from the amplitude of the *g* 1.94 line at 45 °K. In ETP_H samples without rotenone, the overlap from the signals of succinate dehydrogenase (S-1 and S-2) was corrected by subtracting the amplitude of succinate-treated ETP_H. Signals from S-1 and S-2 were not present in the presence of DB. N-2 was estimated from the area under the *g* 2.054 line at 16 K. Reduction of N-3 ($g_{x,y,z}$, 1.86, 1.93,2.04, Ohnishi's terminology (2)) and N-4 ($g_{x,y,z}$, 1.88, 1.93,2.10) was quantitated by the areas covered by the troughs at *g* 1.86 and *g* 1.88, respectively. N-4 was also determined from the area under the g_z (2.10) line. The g_z line (2.04) of N-3 could not be used for quantitation due to its overlap with other lines (3). The relative concentration of center N-5 (g_z 1.90 and g_x 2.07 (2)) was very low and hence we did not measure this center in our experiments. This center may not be a component of the enzyme since it is not seen in *C. utilis* (31) or plant mitochondria (32). Ohnishi (2) suggested the existence of two types (N-1a and N-1b) of N-1 centers with different midpoint potentials. It was also suggested that only N-1b can be reduced with NADH (6). However, these observations have been questioned (3). Since the relative contributions of the two forms cannot be reliably estimated we treat it as a single component in our experiments.

The rates of electron transfer from NADH to DB, ferricyanide, and juglone (5-hydroxy-1,4-naphthoquinone) were assayed by following the oxidation of NADH fluorometrically. The samples, treated with myxothiazol to block electron transfer through the bc_1 complex, were suspended in 250 mM sucrose, 10 mM K-MOPS, pH 7.5, buffer to a final concentration of 0.1 mg of protein ml^{-1} at 25 °C. After the addition of the acceptor, the reaction was initiated by the addition of NADH (final concentration 8 μM). The initial rate of decrease of NADH fluorescence was taken as the rate of electron transfer to the acceptor used. The concentrations of NADH (8 μM), DB (27 μM), and juglone (15 μM) were higher than the respective K_m values. However the rates were dependent on the concentration of ferricyanide (75 μM) used (K_m for ferricyanide ~3 mM), and hence any change brought about by chemical modification might not represent the change in V_{max}. Electron transfer to DB was sensitive to rotenone (~99% inhibition) and caused proton translocation in ETP_H, showing that DB mimics the physiological electron acceptor ubiquinone (30).

ATP-driven reverse electron transfer from succinate to NAD was monitored by observing the increase in NADH fluorescence. Measurements were made in a 3 mm (inner diameter) EPR tube under conditions identical to those used for experiments detailed in Table II. An Eppendorf fluorometer was used in all the fluorescence measurements. Its optical configuration minimized light scattering due to high concentrations of ETP_H (30 mg ml^{-1}).

Superoxide formation was measured by the superoxide dismutase-sensitive reduction of acetylated cytochrome *c* (33) which was prepared according to Takeshige and Minakami (34). The rates were linear with time, unlike the assay by adrenochrome formation which showed nonlinearity (36). Typically the assay medium contained ETP_H (0.45 mg of protein ml^{-1}) in 250 mM sucrose, 50 mM Tris-Cl, pH 7.5, buffer at 25 °C. The following additions were then made: rotenone (8 μM), myxothiazol (2 μM), KCN (0.5 mM), and acetylated cytochrome *c* (36 μM). Superoxide generation was initiated by the addition of either reduced pyridine nucleotide or ATP. Absorbances at 550 nm or 550–540 nm were recorded using a Cary 219 or an Aminco DW-2 spectrophotometer. In the case of superoxide generation by ATP-driven reverse electron transfer from succinate, rotenone was omitted and the medium also contained succinate (10 mM), $MgCl_2$ (8 mm) and bovine serum albumin (1 mg ml^{-1}). After incubation for 10 min, ATP (2 mm) was added and the absorbance at 550–540 nm was recorded. Myxothiazole prevented O_2^- formation by succinate in the absence of ATP (35). The presence of KCN was required to inhibit the oxidation of the reduced cytochrome *c* by the cytochrome *c* oxidase. Superoxide dismutase (0.1 mg ml^{-1}) used in our experiments was active enough in the presence of 0.5 mM KCN to dismutate the superoxide. This was also checked by the effect of superoxide dismutase on superoxide generated by xanthine and xanthine oxidase.

RESULTS

Inhibitors of Electron Transfer

The Fe-S centers of NADH-Q oxidoreductase (both in complex I and ETP_H) were highly reduced (90% or more) under conditions of steady state electron flux from NADH to DB (Table I). This indicates that the major rate determining step is after all the Fe-S centers, and any inhibition of electron transfer after the Fe-S centers would not alter the reduction levels.

Reaction with PCMBS—Reaction of sulfhydryl reagents with both soluble NADH dehydrogenase and ETP_H has been studied extensively (for a review see Ref. 9). Multiple sites of reaction of mercurials were inferred from different assays. Reaction at some of the sites inhibited the oxidase activity more than the ferricyanide reductase activity. One of the SH groups was shown to be involved in piericidin binding and another was shown to be protected by phosphate. Another SH group was called "the occult SH" since it was accessible only after preconditioning the enzyme with NADH (37).

Reaction of PCMBS at low concentrations (30 μM) with either ETP_H or complex I resulted in loss of electron transfer preferentially to DB (Table I). The reduction levels of the Fe-S centers increased to about 100% suggesting that the major site of inhibition was after all the Fe-S centers. Higher concentrations (150 μM) of PCMBS resulted in progressive loss of EPR signal from center N-4 (g_x 1.88, g_y 1.93, and g_z 2.10) (Fig. 1*B*). The progressive loss of N-4 signal saturated at about 150 μM of PCMBS. Further increase of PCMBS con-

TABLE I

Inhibition of electron transfer rates and the effect on reduction of Fe-S centers in NADH-Q oxidoreductase (complex I) by various reagents.

Treatment with the reagents was carried out at pH 7.5, 25 °C for 30 min except in the cases of PCMBS where the treatments were done at pH 6.5 for maximum reactivity (see text). For other details see "Materials and Methods."

Reagents and conditions used	Rate of electron transfer from NADH to acceptors. Percentage of the rates in the unmodified enzyme[a]			Percentage reduction of Fe-S centers[b]							
				During electron flow from NADH to DB				Reduced with dithionite			
	DB	Juglone	Ferricyanide	N-1	N-2	N-3	N-4	N-1	N-2	N-3	N-4
Without any treatment, pH 7.5	100	100	100	91	100	87	91	100	100	100	100
30 μM PCMBS	20	62	86	115	100	100	100	110	100	100	100
200 μM PCMBS	1	71	43	97	100	153	~0	101	95	161	~0
200 μM PCMBS + DTT added later (2 mM)	38	112	111	109	100	111	102	107	98	113	99
NADH (1 mM) pretreated + 200 μM PCMBS	2	11	9	7	<10	<10	~0	115	100	129	0
N-Bromosuccinimide (80 μM)	80	146	92	86	84	93	16	72	99	102	16
DEPC (1 mM)	6	22	11	74	93	52	41	105	110	105	109
NADH (1 mM) pretreated	60	62	61	21	84	74	73	90	96	70	90
Dinitrodifluorobenzene (0.4 mM)	12	48	67	91	86	83	78	93	95	97	94
Tetranitromethane (1 mM)	9	61	39	69	78	59	58	69	112	116	93
DCCD (0.5 mM)	21	61	66	97	102	98	90	99	101	102	97
p-Azidophenacylbromide (1.0 mM)	10	48	50	78	74	93	80	103	104	98	93

[a] 100% rates of electron transfer were 0.18, 0.38, and 1.2 μmol NADH oxidized min^{-1} mg $protein^{-1}$ at 25 °C with DB, juglone, and ferricyanide, respectively, as acceptors. V_{max} values were in the range of 0.5–0.7 and 150–250 μmol of NADH oxidized min^{-1} mg $protein^{-1}$ with DB and ferricyanide, respectively, under conditions according to Ref. 59.

[b] 100% reduction levels are those when the samples were reduced either by NADH alone or by NADH and dithionite in the presence of mediators.

centration did not have any effect on the shape of the signal. Also, the signal intensity of the *g* 1.86 line of N-3 (g_x 1.86, g_y 1.93, g_z 2.04) increased on treatment with PCMBS. The loss of N-4 signal was not reversed by reduction with dithionite suggesting that N-4 itself, rather than electron transfer to N-4, was affected by PCMBS. Further, the loss of N-4 was not prevented by either rotenone or phosphate (50 mM) which has been shown to protect one of the SH groups (9). The increased intensity of N-3 is probably the result of relieving of spin-spin interaction between N-3 and N-4, suggesting that they are close together (Fig. 5). An alternate suggestion that center N-4 might have been modified such that its signals shifted to the N-3 position is not likely. This is because if the g_x line of N-4 had moved to the g_x position of N-3, then either the *g* 1.93 intensity should have remained unaltered or the g_y line of N-4 should have been shifted in position, contrary to the observations (Fig. 1, *10K section*). Mersalyl had an effect on activity and N-4 similar to that of PCMBS. *N*-Ethylmaleimide had no effect either on the activity or on N-4. The loss of N-4 signal by reaction with PCMBS was higher at lower pH of the reaction medium with half-maximum at pH 7.6 (data not shown). However, the inhibition of electron transfer was not significantly dependent on pH. Treatment of PCMBS-treated complex I with DTT (2 mM for 10 min) restored electron transfer to DB partially and the N-4 signal and other electron transfer activities completely (Fig. 1*C*, Table I). Similar reactivation of activity of mersalyl-treated NADH dehydrogenase by DTT was observed previously (38).

Reaction of PCMBS with NADH-preconditioned complex I inhibited all electron transfer activities to similar extents (Table I) (the occult SH site (37)). Reduction levels of all the Fe-S centers were very low with NADH as reductant as was previously reported for N-1 (*g* 1.94 signal) under these conditions (37). Dithionite restored all the signals except N-4 showing that the site of inhibition is between NADH and all the Fe-S centers. Treatment with DTT did not reverse the effects caused by PCMBS under these conditions.

Previous attempts to measure the location of Fe-S centers in the mitochondrial membrane by paramagnetic probes have not been conclusive. Studies with Ni^{2+} (39) and Dy^{3+} (40) showed no interaction, indicating in the latter case that N-2 and N-3 are buried at least 30 Å within the membrane. PCMBS only slowly permeates biological membranes, however (41), and yet can alter center N-4 from the matrix side. To investigate the sidedness of PCMBS reaction with N-4, we compared the reaction of PCMBS with ETP_H and well-coupled beef heart mitochondria (Fig. 2). The data clearly show the accessibility of N-4 to PCMBS in ETP_H but not in mitochondria. Reaction with PCMBS at high concentrations (>200 μM) with ETP_H resulted in partial loss of signals from N-2 and N-1 also (Fig. 2). Under these conditions much less effect was noted in mitochondria suggesting that most of the Fe-S centers are accessible from the M-side. Reduction of PCMBS-treated ETP_H and mitochondria with dithionite showed the absence of a *g* 1.94 signal from S-1 and S-2 in the case of ETP_H only indicating the accessibility to PCMBS, of the Fe-S centers (S-1 and S-2) of succinate dehydrogenase in ETP_H, but not in mitochondria.

Our results have revealed the presence of at least three sites of PCMBS reaction. One lies after all the Fe-S centers and reaction at this site inhibited electron flow to DB preferentially. Reaction at another site was associated with the loss of N-4 signal. The third site (occult SH group (37)) is on the substrate side of all the Fe-S centers. These three sites could

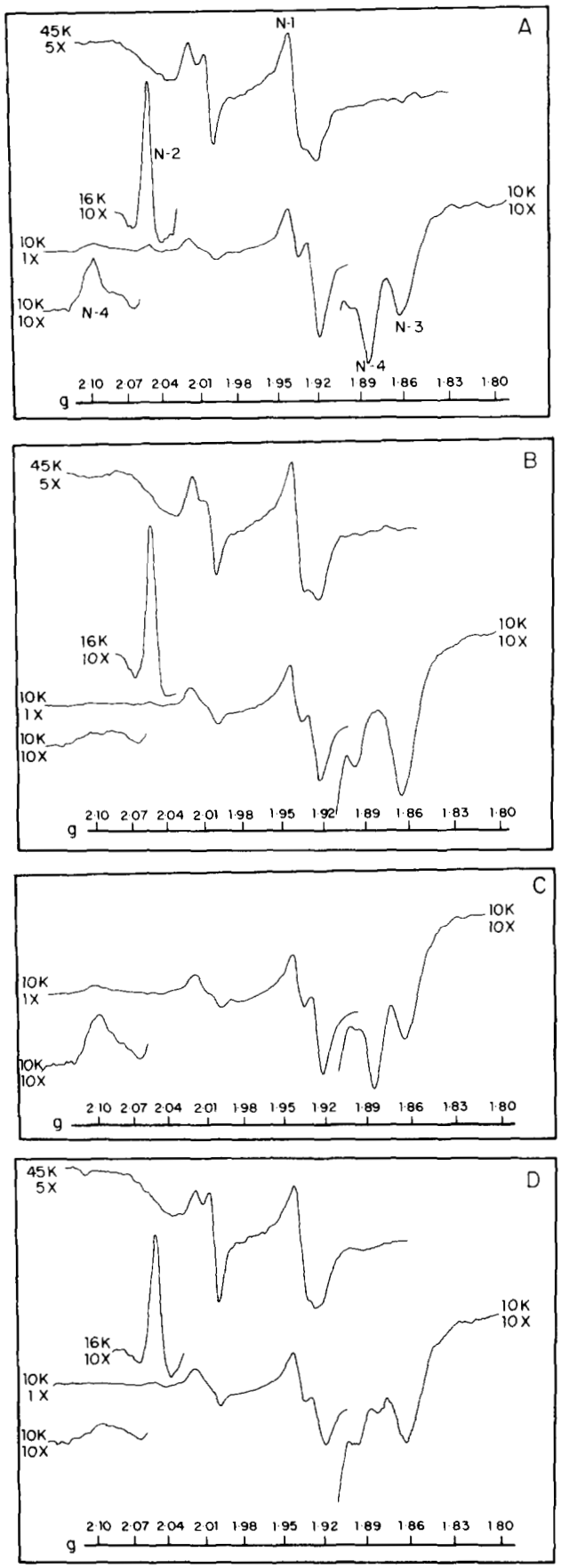

FIG. 1. **EPR spectra of complex I during steady state electron flow from NADH to DB quinone.** *A*, untreated complex I; *B*, complex I treated with 150 μM PCMBS at pH 6.5; *C*, complex I treated with 150 μM PCMB at pH 6.5 and then with 2 mM DTT, and *D*, complex I treated with 80 μM NBS. In *B* and *D* the prominent troughs low field to *g* 1.86 signal is from N-5 (2, 3). EPR conditions were as follows: modulation amplitude 6.3 gauss, microwave power 2 mW. Scan rates and time constants were 250 gauss min^{-1} and 0.5 s for spectra with gain 1 or 5 × and 62.5 gauss min^{-1} and 2.0 s for spectra with gain 10 ×. The temperatures and gains are specified. The protein concentration was 18 mg·ml^{-1}. For other experimental details see "Materials and Methods."

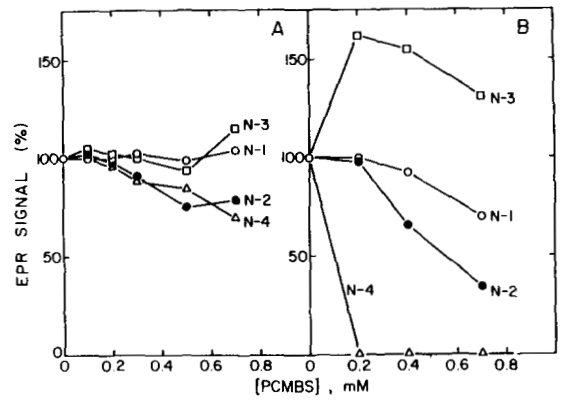

FIG. 2. **Effect of PCMBS on Fe-S centers (N-1 (○), N-2 (●), N-3 (□), and N-4 (△)) in intact mitochondria (*A*) and ETP_H (*B*).** Mitochondria and ETP_H (1 mg of protein ml^{-1}) were treated with PCMBS at 4 °C for 30 min in 250 mM sucrose, 10 mM K-MES, pH 6.5. The excess reagent was removed by centrifugation and the pellet suspended in 250 mM sucrose, 10 mM K-MOPS, pH 7.5, buffer to a protein concentration of ~30 mg ml^{-1}. The mitochondrial samples were then sonicated in a bath type sonicator for 2 min. The samples were then treated with myxothiazol (0.6 g·mg $protein^{-1}$) and DB (2 mM) at 25 °C. NADH (2 mM) was added and samples were frozen, within ~5 s. EPR measurement conditions were as in Fig. 1.

correspond to the three types of SH groups assayed in particulate preparations of the enzyme (9). The presence of multiple sites of reaction of PCMBS does not affect our conclusions, however.

Reaction with N-Bromosuccinimide (NBS)—NBS, which oxidizes tryptophan residues (42) reacted with ETP_H, complex I, and mitochondria resulting in the loss of N-4 signal as well as inhibition of electron transfer activities (Fig. 1*D*, Table I). During titration with NBS the loss of N-4 signal occurred before significant inhibition of electron transfer rates (Fig. 3). At 100 μM NBS, N-4 was ~90% lost with only 40% inhibition of electron transfer to DB. The remaining activity was still rotenone sensitive. The N-4 signal was not restored even when the sample was reduced by dithionite or when treated with DTT + dithionite. When the concentration of NBS was increased, electron transfer to DB was preferentially inhibited (Fig. 3*A*) and the other Fe-S centers were also affected. N-3 was less susceptible to NBS than the other centers (Fig. 3*B*).

The observation that N-4 could be irreversibly lost without significant inhibition of rotenone-sensitive electron transfer to DB suggests a nonlinear arrangement of Fe-S centers (Fig. 5*A*). Center N-4 could be in a side pathway in equilibrium with the main pathway. The observed reduction of N-2 ($E_{m,7.5}$ ~ −30 mV) during electron flow to DB when N-4 ($E_{m,7.5}$ ~ −280 mV) was >95% destroyed by NBS also supports this possibility. Reaction of well-coupled ETP_H with 80 μM NBS (sufficient to cause a 5-fold decrease in the N-4 signal with only 20% inhibition of electron flow to DB) did not affect proton translocation coupled to electron transfer to DB as observed in NADH pulse experiments (data not shown). This suggests that modification of N-4 by NBS does not affect energy coupling also. It must be pointed out, however, that

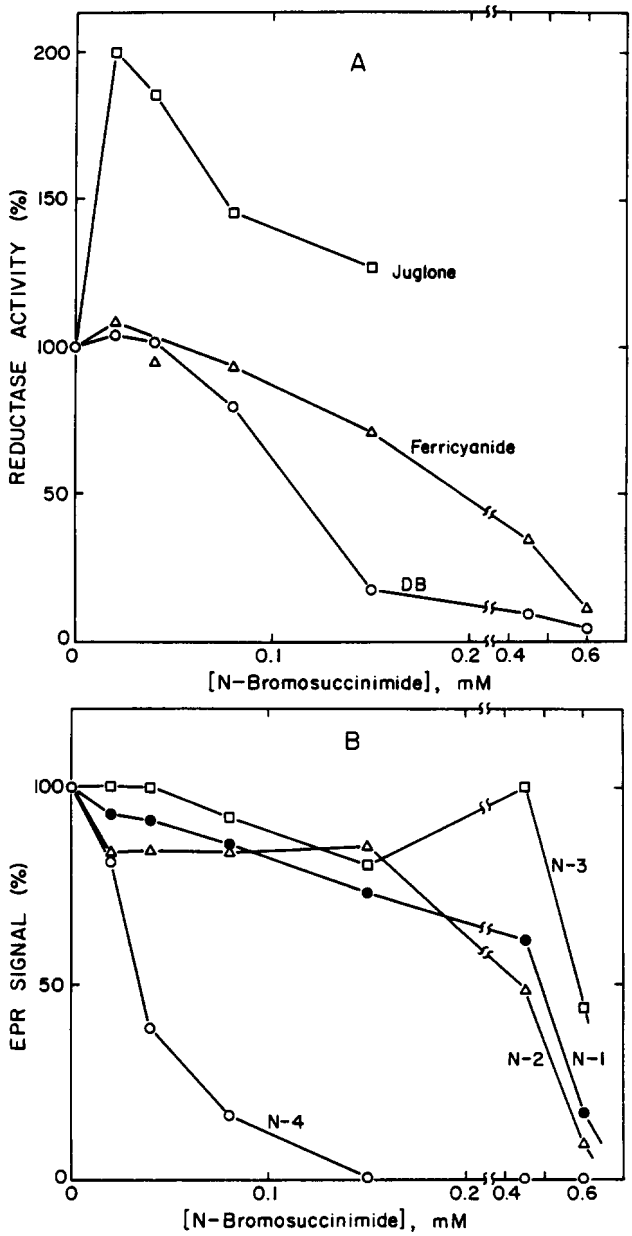

FIG. 3. *A*, dependence of the rate of electron transfer from NADH to DB (○), ferricyanide (△), and juglone (□) on the concentration of *N*-bromosuccinimide in ETP_H. Reaction with *N*-bromosuccinimide and measurement of electron transfer rates were carried out as described under "Materials and Methods." *B*, effect of *N*-bromosuccinimide treatment on the Fe-S centers (N-1 (○), N-2 (△), N-3 (□), and N-4 (○)) in ETP_H. After reaction with *N*-bromosuccinimide, ETP_H samples were treated with myxothiazol and DB and reduced with NADH as described under "Materials and Methods." Quantitation of Fe-S centers from the EPR spectra is also detailed in that section.

the absence of N-4 signal in the temperature range (4–45 K) of our EPR measurements does not prove its nonfunctionality as an electron carrier. It is possible that N-4 was modified such that it became EPR silent but still behaved normally as an electron carrier. The irreversible and specific loss of Fe-S signals by reaction with NBS (Fig. 3) could be useful in assigning the Fe-S centers to the resolved fractions of complex I (14, 15).

Reaction with DEPC—DEPC, a reagent for histidine (43) strongly inhibited all electron transfer activities (Table I) similar to earlier observations (44). During steady state electron flow to DB, there was less reduction of N-3 and N-4 than of N-1 and N-2 suggesting that DEPC blocked the electron transfer from N-1 to N-3 and N-4. The higher reduction level of N-2 could be due to its higher midpoint potential ($E_{m,7} \sim -30$ mV). The reduction levels of all the Fe-S centers were restored to near 100% when the sample was reduced by NADH in the absence of DB or by dithionite.

These results suggest the presence of a histidine residue(s) essential for electron transfer from NADH to any of the acceptors used for electron flow from N-1 to N-3 and N-4. Also they place N-1 before N-3 and N-4 in the electron transfer pathway.

Reaction with other Reagents—Reaction with tetranitromethane, a tyrosine reagent (43), resulted in preferential inhibition of electron transfer to DB (Table I). After tetranitromethane treatment, N-3 and N-4 were less reduced than N-1 and N-2 during electron transfer to DB. However, reduction with dithionite restored N-3 and N-4 reduction levels to unmodified values. These results support the conclusion that N-1 is located before N-3 and N-4 in the reaction sequence.

The cross-linking agent, difluorodinitrobenzene, the carboxyl reagent dicyclohexylcarbodiimide (DCCD), and amino group reagents *p*-azidophenacyl-bromide, fluorodinitrobenzene, and *N*-nitrophenylsulfenylchloride reacted with ETP_H and complex I resulting in preferential inhibition of electron flow to DB. Similar inhibition by DCCD has been observed by others (45, 46). The reduction levels of the Fe-S centers were not altered by these reagents (Table I), indicating that the rotenone-like inhibition was due to reactions at sites after all the Fe-S centers.

Phillips and Kell (47) observed growth inhibition of rotenone-insensitive *Paracoccus denitrificians* cells by Tinopal AN (1,1-bis(3,*N*-5-dimethylbenzoxaol-2-yl)-methine-*p*-toluene sulfonate), and suggested that Tinopal AN might bind at a site different from that of rotenone. We observed that Tinopal AN inhibited electron transfer preferentially to DB. At 22 μg/mg protein, we observed 86, 45, and 53% inhibition of electron transfer to DB, juglone, and ferricyanide respectively. EPR measurements indicated that Tinopal AN had no effect on the reduction level of Fe-S centers during DB reduction. Thus, there are probably multiple sites of inhibition, the major site being similar to rotenone.

Local anesthetics like butacaine also inhibit NADH-Q oxidoreductase (48). We found that butacaine inhibited electron transfer to DB preferentially, without altering the reduction of any of the Fe-S centers indicating that butacaine might bind at a site after all the Fe-S centers.

Prolonged incubation with NADH was shown to affect center N-1 (7). We obtained similar results (Table I). Treatment of complex I with 1 mM NADH at 25 °C for 30 min resulted in a pronounced decrease in the N-1 signal during electron flow to DB. The reduction levels of other Fe-S centers were also slightly lowered. Electron transfer activities with all the acceptors were inhibited to similar extents. However, N-1 and other Fe-S centers showed complete reduction when reduced by dithionite (Table I) indicating that the decrease in the signals of N-1 and other centers was caused mainly by the blockage of electron transfer from NADH. Tyler (49) suggested that superoxide generated during preconditioning with NADH could be the cause of inactivation of the enzyme.

Effect of ATP Energization on the Reduction Levels of Fe-S Centers

Equilibration with the NADH/NAD Couple—Addition of ATP to well-coupled ETP_H had no effect on the measured reduction levels of any of the Fe-S centers when equilibrated

with the NADH/NAD couple (Table II). The ratio of NADH/NAD was varied from 100 to 0.01. Centers N-1, N-3, and N-4 were titratable in this range and their apparent midpoint potentials are given in Table II. N-2 ($E_{m,7.5}$ = −30 mV) remained fully reduced in all the samples, as expected.

The absence of any effect of the addition of ATP was observed even when the medium contained either ammonium sulfate (10 mM) or sodium perchlorate (10 mM) (data not shown). These agents are known to increase $\Delta\psi$ and ΔpH, respectively, at the cost of the other component. Complications due to possible artifacts caused by competitive inhibition of NADH dehydrogenase by ATP (50) were overcome by comparing the samples with ATP in the presence and absence of uncoupler (Table II). Gutman *et al.* (20) reported reduction of N-1 by ATP in piericidin-treated ETP_H using NADH/NAD redox buffer. No change in the reduction levels of other low potential centers was seen in their data. On the other hand, Ingledew and Ohnishi (6) reported ATP-induced oxidation of N-4 but not other centers, in pigeon heart submitochondrial particles under similar conditions. Why our results (Table II) are different from these, is not clear. Gutman *et al.* (19) showed ATP-induced oxidation of N-2 in piericidin-treated ETP_H. However, their experimental system was not well defined in terms of the potential clamped by the NADH/NAD couple. In their method, added NADH was allowed to oxidize completely through the piericidin block. N-2 remained reduced under these conditions and addition of ATP caused oxidation of N-2. In all measurements of ATP-driven reverse electron transfer to NAD, there is probably some rapid reequilibration of electrons due to decay of $\Delta\psi$ during freezing of the sample for EPR measurements (see "Discussion").

Equilibration with the Succinate/Fumarate Couple—ATP can cause reverse flow of electrons from succinate to NADH (51). This reaction has been useful as a method for estimating the coupling ratios for this site (21, 22, 24). It is interesting to ask whether ATP can cause reduction of the low potential Fe-S centers in ETP_H equilibrated with the succinate/fumarate couple in the absence of NAD. Table II shows that ATP can indeed cause uncoupler-sensitive reduction of N-1, N-3, and N-4 with succinate/fumarate buffer in the absence of NAD. The reduction of N-3 and N-4 was more prominent than that of N-1. The reduction level of N-2 increased only slightly in accordance with the results of Gutman *et al.* (20). From a knowledge of the midpoint potentials of the Fe-S centers (Table II) and ATP-induced reduction levels of the centers (Table II), we can estimate the apparent potentials (E_h) imposed at the Fe-S centers by ATP energization as about −230, −270, −260, and −50 mV at N-1, N-3, N-4, and N-2, respectively, when the redox potential clamped by succinate/fumarate was −30 mV.

ATP-driven reverse electron flow caused ~60% reduction of NAD in ETP_H samples (see "Materials and Methods"). In the presence of NAD, we also observed a significant increase in ATP-driven reduction of the Fe-S centers (Table II). Structural changes caused by the binding of NAD could be one possible cause of this effect. Alternatively, the increased reduction in the presence of NAD could result from a "U-turn" or branching. The samples of ETP_H had about 40% of noncoupled enzyme such as incorrectly oriented complexes or permeant vesicles. (The existence of a noncoupled enzyme population is indicated from the effect of polylysine on NADH-respiration. Polylysine inhibits cytochrome oxidase by binding at the cytochrome *c* site (52) which is accessible in noncoupled vesicles only. Polylysine inhibited both controlled and uncoupled respiration in our ETP_H samples resulting in an increase of the respiratory control ratio from 2.5 to 8.5. From the respiratory control ratio in the absence of polylysine we estimate that our samples had about 40% of noncoupled enzyme.) The NADH formed by the coupled enzyme would reduce the noncoupled enzyme resulting in higher reduction levels in the presence of NAD. Correction for the noncoupled population leads to ATP-induced potentials felt at the Fe-S centers as −254, −295, −285, and −60 mV for N-1, N-3, N-4, and N-2, respectively, when the potential clamped by the succinate/fumarate couple was −30 mV. The potential felt by NADH was about −325 mV under these

TABLE II

Effect of ATP energization on the reduction levels of Fe-S centers in ETP_H equilibrated with either NADH/NAD buffer (forward reaction) or succinate/fumarate buffer (reverse reaction)

For the forward reaction, 0.28 ml of ETP_H (30 mg·ml^{-1}), suspended in 250 mM sucrose, 10 mM K-MOPS, pH 7.5 buffer was treated with 540 μM rotenone for 30 min at 0 °C. The sample was then thermostated at 25 °C and the following additions were made (final concentrations indicated in parentheses); $MgCl_2$ (12 mM), bovine serum albumin (1 mg·ml^{-1}), creatine phosphokinase (20 μg·ml^{-1}) and NAD (0.01–8.0 mM). The sample was then transferred into EPR tubes and NADH (0.08–4.0 mM), phosphocreatine (10 mM), and (ATP 0.7 or 10.0 mM) were all added at once. 20 s after the addition, the sample was quickly frozen in a 1:5 mixture of methyl-cyclohexane-iso-pentane cooled in liquid nitrogen. For the reverse electron transfer, rotenone was replaced by myxothiazol (14 μg·ml^{-1}) and KCN (6 mM). The samples were incubated with succinate (9 mM) for 10 min at 25 °C in order to activate succinate dehydrogenase. Fumarate (0.9 mM) was then added. Other additions were as before. In samples with NAD, NAD (0.25 mM) was added before myxothiazol treatment. Conditions for EPR measurements were as given under "Materials and Methods" and in Fig. 1. The symbols −U and +U designate samples without and with uncoupler (70 μM 3,5-di-*tert*-butyl-4-hydroxybenzylidenemalanonitrile), respectively.

Redox component	$E_{m,7.5}$[a]	Reduction level %							
		Equilibrated with NADH/NAD				Equilibrated with succinate/fumarate E_h = −30 mV			
		E_h = −333 mV		E_h = −280 mV					
		−U	+U	−U	+U	−U	+U	−U +NAD	+U +NAD
	mV								
NADH/NAD	−320							60	0
N-1	−318	63	70	32	29	10	~0	22	~0
N-2	−30	100	100	100	100	69	56	100	83
N-3	−265	86	95	77	68	54	20	100	20
N-4	−285	79	73	48	52	36	10	47	15

[a] $E_{m,7.5}$ values were obtained by tritration with either NADH/NAD or succinate/fumarate couples.

conditions. These values, which are similar to the uncorrected values given above, indicate the presence of a major coupling interaction between N-2 and the low potential centers and minor coupling effects between N-2 and the quinone-binding site and between NADH and the low potential centers. Gutman *et al.* (20) claimed ATP induced reduction of N-1 with succinate/fumarate buffer. However, the presence of NAD in their system does not allow one to distinguish whether the observed reduction was due to ATP-induced potential felt by N-1 in the coupled enzyme or due to NADH reducing the noncoupled enzyme. Moreover, they did not measure the other low potential centers.

Superoxide (O_2^-) Production in ETP_H—The redox characteristics of FMN in NADH-Q oxidoreductase are unknown due to spectral overlap of Fe-S centers. An early study by Hinkle *et al.* (53) showed than an autoxidizable component on the substrate side of the coupling site in NADH-Q oxidoreductase generates H_2O_2. Later studies (34, 35, 54, 55) on O_2^- (a precursor of H_2O_2) generation, however, were not aimed at locating the site exactly. Flavoenzymes are known to generate O_2^- (56). If FMN is the site of O_2^- generation then one could monitor the redox state of FMN from the rate of O_2^- generation. Our measurements were confined to rotenone-treated ETP_H, and hence the quinone site of O_2^- generation (54, 57, 58) was excluded in our observations.

Titrations with NADH/NAD Couple—In the presence of NADH, rotenone-treated ETP_H generated 0.9 nmol of O_2^- min^{-1} mg $protein^{-1}$ at pH 7.6 as detected by 36 μM acetyl cytochrome *c*. This rate was dependent on the concentration of acetyl cytochrome *c* and reached a maximum of about 2 nmol min^{-1} mg of protein at very high concentrations of acetyl cytochrome *c*. NAD inhibited the NADH-dependent O_2^- generation. This inhibition is similar to the inhibition of ferricyanide reductase activity of NADH-dehydrogenase by NAD (59). The rate was dependent on the ratio [NADH]/[NAD] rather than on the concentration of NADH and NAD. The data in Fig. 4 show that the rate increased with increasing values of [NADH]/[NAD]. The rate increased linearly with ETP_H concentration. The titration curves (Fig. 4, *A–C*) were very similar in the pH range 6.8–8.4 except for the increase in the absolute values of the rates with increasing pH (54). Half-maximal rates were observed around a value of 0.5 for log [NADH]/[NAD] at all the pH values shown in Fig. 4, *A–C*. If we take the curves in Fig. 4 (*A–C*) to represent titration of a redox component, then its midpoint potential (E_m) would be ~−320 mV at pH 6.8 with 30 mV/pH decrease in its E_m. (This is because of the 30 mV/pH decrease in the E_m of the NADH/NAD couple.)

Titration with APADH/APAD Couple—In order to check whether the rate of O_2^- generation depends on the E_h imposed or on the ratio of reduced nucleotide to the oxidized form, we carried out a titration with the 3-acetyl pyridine adenine dinucleotide (APADH/APAD) couple whose E_m is −248 mV (60). The results (Fig. 4*D*) show that the rate of O_2^- generation depended on the ratio [APADH]/[APAD] in a manner very similar to that seen with the NADH/NAD couple (Fig. 4, *A–C*). The half-maximal rate was observed around a value of 0.3 for log [APADH]/[APAD]. The titration of the Fe-S centers by the APADH/APAD couple showed the lower reducing power of the couple as expected. 71% of center N-4 was reduced at [NADH] = [NAD] = 2 mM whereas only 37% was reduced at [APADH] = [APAD] = 2 mM. The rate of O_2^- generation was about 30–40% of that observed with the NADH/NAD couple at all comparable ratios. This shows clearly that the rate is not a function of the E_h imposed but is dependent on the nature of the reductant and the ratio of

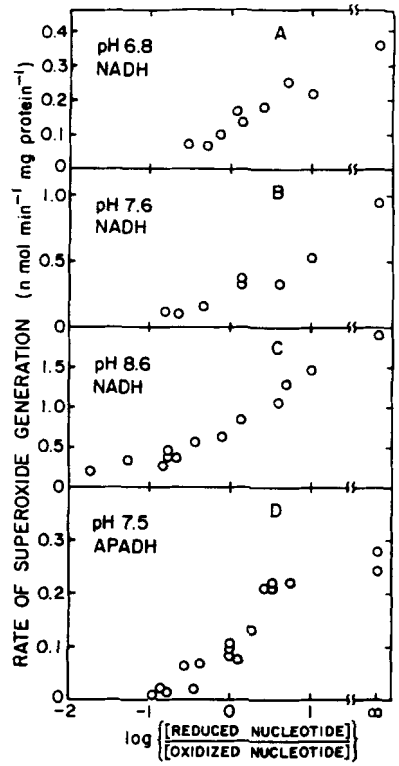

FIG. 4. **Dependence of the rate of superoxide generation by ETP_H on the ratio of [NADH]/[NAD] at pH 6.8 (*A*), 7.6 (*B*), and 8.6 (*C*) and on the ratio of [APADH]/[APAD] at pH 7.5 (*D*).** [NADH] and [APADH] were varied from 30 to 100 μM and [NAD] and [APAD] were varied from 0 to 900 μM. 50 mM MES buffer was used for pH 6.8, and 50 mM Tris for pH 7.5–8.6. For other experimental conditions see "Materials and Methods." Note the difference in ordinate scales.

reduced to oxidized nucleotide. A 3–5-fold lower rate was also observed with NADPH, supporting this conclusion (data not shown).

Effect of Inhibitors—To further characterize the site of O_2^- generation, we used inhibitors mentioned in a previous section. A comparison of the rate of O_2^- generation with other electron transfer activities after reaction with inhibitors is shown in Table III. The inhibition of O_2^- generation was very similar to the inhibition of electron transfer to ferricyanide rather than to DB quinone. Since the site of electron donation to ferricyanide is before the coupling site, the site of O_2^- generation also should be before the coupling site. The higher levels of inhibition observed in ferricyanide activity when compared to the inhibition of O_2^- generation could be due to about 1000-fold higher value of the former when compared to the O_2^- rate in uninhibited samples. The inhibition data supports the contention that O_2^- is generated by the interaction of NADH with NADH-CoQ oxidoreductase and not any other dehydrogenase present as a contamination (also see below).

O_2^- Generation by Reverse Electron Transfer from Succinate—The rate of O_2^- generation in ETP_H by ATP-driven reverse electron transfer from succinate was only about 16% of that observed with NADH as reductant (Table IV). ATP did not inhibit NADH-dependent O_2^- formation (Table IV). The presence of NAD during reverse electron transfer resulted in an increase in the rate of O_2^- generation to about 83% of that observed with NADH (Table IV). Concomitantly, 90–95% of NAD was reduced to NADH. This effect of NAD was independent of its concentration in the range 1 to 70 μM.

TABLE III

Inhibition of superoxide generation and electron transfer from NADH to different acceptors by reaction of ETP_H with various reagents

ETP_H (1 mg of protein ml^{-1}) suspended in 250 mM sucrose, 10 mM K-MOPS, pH 7.5, buffer was treated with the reagent for 30 min at 25 °C. The excess reagent was removed by centrifugation and the pellet suspended in the same buffer. The rate of superoxide generation by NADH (100 μM) was measured as detailed under "Materials and Methods."

Treatment with reagents	Rate of electron transfer from NADH to acceptors[a]		Rate of O_2^- generation[b]
	DB	Ferricyanide	
	% of unmodified		% of unmodified
Rotenone	0	100	100
N-Bromosuccinimide (0.3 mM)	9	72	84
p-Chloromercuribenzene sulfonate, 0.2 mM	15	67	66
NADH (1 mM) pretreated	50	54	63
NADH (1 mM) pretreated + *p*-Chloromercuribenzene-sulfonate (0.2 mM)	2	4	26
DEPC (mM)	6	22	26
DCCD (1 mM)	17	73	57
Tetranitromethane (1 mM)	10	35	48
p-Azidophenocylbromide (1 mM)	24	55	48

[a] 100% rates of electron transfer were 0.19, and 1.03 μmol of NADH oxidized min^{-1} mg $protein^{-1}$ at 25 °C with DB, and ferricyanide, respectively, as acceptors.

[b] 100% rate of O_2^- generation was 0.90 nmol min^{-1} mg $protein^{-1}$.

TABLE IV

Rates of generation of superoxide by ETP_H during forward and ATP-driven reverse electron transfer

For details see "Materials and Methods." SF 6847, 3,5-di-*tert*-butyl-4-hydroxybenzylidenemalanonitrile

Conditions used	Rate of O_2^- generation[a]
	%
ETP_H + Rotenone + NADH	100
ETP_H + myxothiazol + succinate + ATP	16
ETP_H + myxothiazol + succinate + NAD (70 μM) + ATP	83
ETP_H + myxothiazol + SF 6847 + succinate + ATP	0
ETP_H + myxothiazol + SF 6847 + succinate + ATP + NADH	98

[a] Measured at 37 μM of acetylated cytochrome *c*. 100% rate was 0.90 nmol min^{-1} mg $protein^{-1}$.

However, NAD did not have appreciable effect on the ATP-driven reduction of ferricyanide by succinate. The enhancement in the rate was at best by a factor of 1.6 (at 50 μM ferricyanide and 2 mM NAD). Previous studies (36) on O_2^- production during reverse electron flow at this site have not been carried out in the absence of NAD.

The 5-fold increase in the rate of O_2^- production in the presence of added NAD cannot be explained by the presence of noncoupled enzyme population which would be reduced by the NADH formed by the coupled enzyme. Our ETP_H preparations had about 40% of noncoupled enzyme, and hence NAD would be expected to increase the rate by less than 2-fold only. Also, the above-mentioned enhancement by NAD would be expected if some other NADH-induced O_2^--generating system is present as a contamination. Lipoamide dehydrogenase (diaphorase) which is very efficient in NADH-induced O_2^- production (20 nmol min^{-1} mg $protein^{-1}$) is an attractive possibility. However, assay of our ETP_H sample showed less than 1% activity of lipoamide dehydrogenase when expressed in terms of activity/mg of protein. Hence the 5-fold increase in the rate of O_2^- generation on addition of NAD most probably shows a requirement for bound pyridine nucleotide for O_2^- generation.

Bound Nucleotide As the Site of O_2^- Generation—The experiments described in this section suggest that bound reduced pyridine nucleotide is the major source of O_2^- generation in rotenone-blocked NADH-Q oxidoreductase. This conclusion is arrived at by (i) the similarity in the dependence of the rate of O_2^- generation on the ratios [NADH]/[NAD] and [APADH]/[APAD] (Fig. 4), (ii) the 5-fold increase in the rate during reverse electron flow from succinate in the presence of NAD, and (iii) different rates observed with NADH, NADPH, and APADH which could be due to different stabilities of bound nucleotide. If the flavin (FMN) radical were the site, then we would expect, during titrations with the NADH/NAD couple, a bell-shaped curve similar to that observed at the quinone site (58). This was not observed, indicating that either bound NAD-radical or some complex NAD-FMN radical is the species which reacts with O_2. Formation of O_2^- by the oxidation of bound NAD· radical has been proposed in other dehydrogenases (61, 62). According to this scheme, the rate would be proportional to [*E*-NAD·]. It can be shown that [*E*-NAD·] is proportional to [NADH]/([NADH] + *n* [NAD]) when [NADH], [NAD] >> $[E]_{tot}$, $[E]_{tot}$ being the total concentration of the enzyme. $n = K_1/K_2$, where K_1 and K_2 are dissociation constants associated with the binding of NADH and NAD, respectively. It was assumed that [*E*-NAD·] << [*E*-NADH]. The data in Fig. 4 could be fitted to the following equation

$$\text{rate, } [O_2^-] \text{ generation} = \frac{K\,[\text{NADH}]}{[\text{NADH}] + n[\text{NAD}]} \quad (1)$$

with *n* in the range of unity.

Free Radical Species in Complex I and ETP_H

NADH-reduced complex I and ETP_H had a narrow EPR resonance at *g* 2.00 indicating the presence of free radical(s). Addition of low levels (similar to the concentration of enzyme) of NADH to complex I caused a free radical signal which decreased in amplitude at higher concentrations of NADH (data not shown). This observation was similar to that of Orme-Johnson *et al.* (7). The *g* 2.00 signal was unchanged by rotenone, thereby eliminating Q· (63) as the source of the signal. Direct correlation between the signal and either the flavin radical or the *E*-NAD· radical was not possible since the amplitude of the signal did not depend significantly on the NADH/NAD ratio. However, the signal may originate from a combination of these two radicals. Also, during steady state electron flow from NADH to DB, in well-coupled ETP_H, uncouplers caused a 35% decrease in the amplitude of the *g* 2.00 signal. No change in the signals of Fe-S centers were observed.

DISCUSSION

Several conclusions can be drawn from the current studies, although the exact pathway of electrons from NADH to Q is still elusive. The reversible loss of center N-4 on treatment of ETP_H with PCMBS did not occur when mitochondria were similarly treated, indicating that N-4 is located on the matrix side of the membrane. Further, this experiment also showed that N-2 and N-1 are also more accessible from the M-side.

The concomitant increase in the N-3 signal when N-4 was destroyed by PCMBS suggests spin coupling between the two centers. Alternatively, the increase in the amplitude of the N-3 signal could be due to relieving of interaction with some other paramagnet. Ohnishi and co-workers (2, 6) proposed spin-spin interaction between N-3 and an FMN radical from an NADH/NAD titration of N-3 in pigeon heart submitochondrial particles. However, we did not observe such an interaction (anomalous dip around −350 mV in the titration curve) in our experiments (data not shown). The loss of N-4 signal without inhibition of electron transport which occurred with NBS treatment suggests that N-4 is on a side pathway of electron transfer which may serve a buffering function. The inhibition by DEPC and tetranitromethane suggests that N-1 lies before N-3 and N-4 which is consistent with the lower E_m of N-1.

Recently, Bakker and Albracht (8) have suggested a linear pathway of electron flow through Fe-S clusters from pre-steady state kinetics of reduction of ETP_H by NADPH and reoxidation of the reduced enzyme (8). Their proposed arrangement of Fe-S clusters is similar to the sequence based on their midpoint potentials (Table II). (We follow Ohnishi's terminology (2) which is the reverse of Albracht's for N-3 and N-4.) However, this need not represent the actual sequence of electron flow, since their results could also be explained as the outcome of a rapid potentiometric titration. Further, they proposed a dimeric model for some of the Fe-S clusters. Although our work is not aimed at answering this question, the monophasic decrease in N-4 signal intensity when reacted with NBS (Fig. 3*B*) suggests the presence of only one type of this cluster.

Our current working hypothesis which incorporates the above findings is shown in Fig. 5*A*. A cleft on the M side allows access of PCMB and NBS to Fe-S center N4. This cleft is shown as the site of interaction of NADH and $Fe(CN)_6^{3-}$ which compete with each other, indicating a common access site (64). A second cleft from the M side allows access of protons and PCMBS to the site where N2 reduces Q. A proton channel is shown leading from the C side to the flavin site. This channel is necessary because the flavin is tightly bound. It is not permeated by PCMBS or ferricyanide.

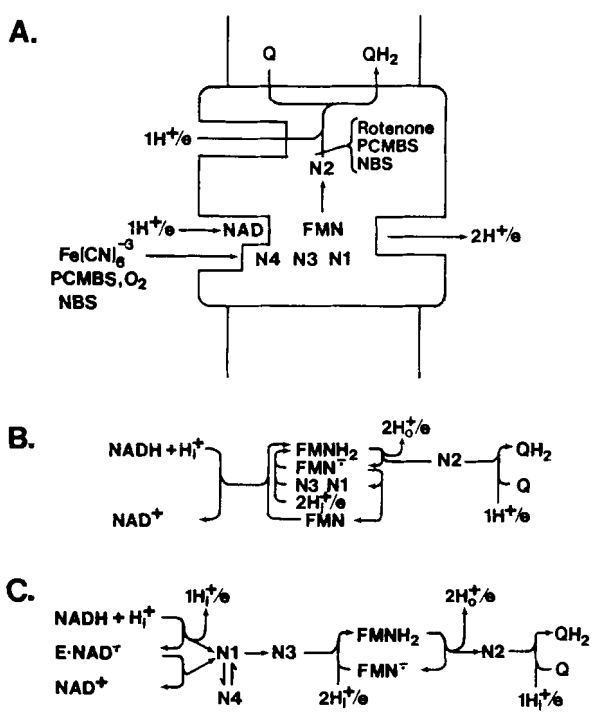

FIG. 5. **Schemes for proton transport at site 1 discussed in the text.** *A*, locations of components in complex I consistent with *B* and *C*. *B*, flavin cycle, analogous to the "b-cycle" proposed for site 2 (65). *C*, single electron transfer from NADH.

The rough picture of locations of components in Fig. 5*A* is compatible with many schemes of electron and proton flow, but we favor those shown in Fig. 5, *B* and *C*. Fig. 5*B* shows a scheme very similar to the "b-cycle" at site 2 (65) but with flavin and Fe-S centers in place of Q and *b* cytochromes. It is best understood by considering two catalytic cycles. The first mole of NADH reduces FMN to $FMNH_2$ which then donates one electron to N-2 and another to the N-1, N-3, N-4 group of Fe-S centers, releasing two protons on the C-side. Center N-2 then reduces Q absorbing one proton on the M side. The complex is now in a different state from the start because an electron is left in the N-1, N-3, N-4 centers. The second molecule of NADH now reduces FMN to $FMNH_2$ as before, but now $FMNH_2$ passes one electron to N-2 forming $FMN^{\cdot}$ and releasing two protons to the C side. N-2 reduces Q, absorbing one proton from the M side. The $FMN^{\cdot}$ is now reduced with the electron from the group N-1, N-3, and N-4 forming $FMNH_2$ and absorbing two protons from the M side. At this point the system is in the same state as that formed by the initial reduction of FMN to $FMNH_2$ by NADH and the four protons transported are the result of two electrons passing through the system. This coupling ratio of $4H^+/2e$ is indicated by several recent studies (21–25), although one group claims it is as high as 5 (25), and another that it is 3 (22). When the fact that the substrate is NADH + H^+ is taken into account the stoichiometry/electron pair is $-5H^+$ inside mitochondria (M side), $+4H^+$ outside mitochondria (C side), which we call $4H^+/2e$ for simplicity.

The scheme in Fig. 5*B* requires that the half-reduced flavin be fully ionized. The pK_a of free $FMN^{\cdot}H$ is ~8.5 (66) so the binding site would have to lower this value by local position change or other means. Similarly, the fully reduced flavin, $FMNH_2$, must be fully protonated. The pK_a of free $FMNH_2$ is 6.5 (66) which would have to be raised by the binding site. The scheme has the advantage that it uses FMN as a transformer from the two-electron carrier NADH to one-electron carriers. It predicts several unusual properties of electron flow which have not been observed, such as limited reduction of centers N-1, N-3, N-4 when N-2 oxidation is blocked by rotenone, but the specificity of the reactions does not need to be complete, and the maximum rates of electron flow within the complex have never been measured. We have not included any Q-cycle type complexity in the proposed reduction of Q by N-2 because the midpoint potential of N-2 (−30 mV) is close to the potential of the Q pool, and there is no energy available for any additional proton transport functions at site 1. The reduction of Q one electron at a time would simply absorb protons from the M side to form QH_2.

Fig. 5*C* shows another scheme that could account for the transport of $4H^+/2e$, and involves bound half-reduced NAD ($NAD^{\cdot}$) suggested by our studies of O_2^- formation. In this scheme electrons from NADH are passed directly to the low potential Fe-S group (N-1, N-3, and N-4) and then reduce $FMN^{\cdot}$ to $FMNH_2$, absorbing two protons from the M side/electron and forming one $H^+/2e$ on the M side. The oxidation of $FMNH_2$ by the center N-2 releases $2H^+/e$ on the C side and reduction of Q by N2 absorbs $1H^+/e$. The overall result is the same as for Fig. 5*B*.

The formation of bound $NAD^{\cdot}$ shown by Fig. 5*C* is consistent with the requirement of NAD/NADH for superoxide formation from reverse electron flow at site 1 (Table IV). It

is also possible, however, that the flavin/NAD complex proposed in Fig. 5*B* could be the form reactive with O_2.

Both schemes *B* and *C*, involve free radicals ($FMN^{\cdot}$ and $NAD^{\cdot}$), which are seen by EPR measurement in the steady state and fully reduced state. However, we have not been able to correlate measured values with predictions from the schemes or identify the source of the measured signals.

The effect of ATP on reduction levels of Fe-S centers in coupled ETP_H particles indicated a major coupling interaction between N-2 and all other Fe-S centers when electrons were donated by succinate. When electrons were donated from NADH no effect of ATP was seen, which we attribute to the rapid re-equilibration of electrons during freezing of samples for EPR. The limitation of having to freeze samples for measurements restricts interpretation, and it is likely, for example, that even with succinate as electron donor there is a re-equilibration of the negative Fe-S centers with each other during freezing. The net reduction of the negative centers is preserved during freezing, however, because N-2, Q, and centers in succinate dehydrogenase are all fully reduced by succinate. Thus both schemes *B* and *C* (Fig. 5) are consistent with the results of reverse electron transfer.

Acknowledgments—We thank Dr. L. Que and Dr. J. H. Freed for their generosity in allowing us to use their EPR facility and D. Schneider for his help during the initial phase of the EPR experiments.

REFERENCES

1. Ragan, C. I. (1981) in *Chemiosmotic Proton Circuits in Biological Membranes* (Skulachev, V. P., and Hinkle, P. C., eds) pp. 59–68, Addison-Wesley Publishing Co., Reading, MA
2. Ohnishi, T. (1979) in *Membrane Proteins in Energy Transductions* (Capaldi, R. A., ed) pp. 1–87, Marcel Dekker, New York
3. Beinert, H., and Albracht, S. P. J. (1982) *Biochim. Biophys. Acta* **683,** 245–277
4. Kowall, A. T., Morningstar, J. E., Johnson, M. K., Ramsay, R. R., and Singer, T. P. (1986) *J. Biol. Chem.* **261,** 9239–9245
5. Hatefi, Y. (1985) *Annu. Rev. Biochem.* **54,** 1015–1069
6. Ingledew, W. J., and Ohnishi, T. (1980) *Biochem. J.* **186,** 111–117
7. Orme-Johnson, N. R., Hansen, R. E., and Beinert, H. (1974) *J. Biol. Chem.* **249,** 1922–1927
8. Bakker, P. T. A., and Albracht, S. P. J. (1986) *Biochim. Biophys. Acta* **850,** 413–428
9. Singer, T. P., and Gutman, M. (1971) *Adv. Enzymol.* **34,** 79–153
10. Harmon, H. J., and Crane, F. L. (1976) *Biochim. Biophys. Acta* **440,** 45–58
11. Smith, S., and Ragan, C. I. (1980) *Biochem. J.* **185,** 315–326
12. Cleeter, M. W. J., Banister, S. H., and Ragan, C. I. (1985) *Biochem. J.* **227,** 467–474
13. Gondal, J. A., and Anderson, W. M. (1985) *J. Biol. Chem.* **260,** 12690–12694
14. Ragan, C. I., Galante, Y. M., Hatefi, Y., and Ohnishi, T. (1982) *Biochemistry* **21,** 590–594
15. Ohnishi, T., Ragan, C. I., and Hatefi, Y. (1985) *J. Biol. Chem.* **260,** 2782–2788
16. Chomyn, A., Mariottini, P., Cleeter, M. W. J., Ragan, C. I., Matsumo-Yagi, A., Hatefi, Y., Doolittle, R. F., and Attardi, G. (1985) *Nature* **314,** 592–597
17. Lawford, H. G., and Garland, P. B. (1972) *Biochem. J.* **130,** 1029–1044
18. Ragan, C. I., and Hinkle, P. C. (1975) *J. Biol. Chem.* **250,** 8472–8476
19. Gutman, M., Singer, T. P., and Beinert, H. (1972) *Biochemistry* **11,** 556–562
20. Gutman, M., Beinert, H., and Singer, T. P. (1975) in *Electron Transfer Chains and Oxidative Phosphorylation* (Quagliariello, E., Papa, S., Palmieri, E., Slater, E. C., and Siliprandi, N., eds) pp. 55–62, Elsevier Scientific Publishing Co., New York
21. Rottenberg, H., and Gutman, M. (1977) *Biochemistry* **16,** 3220–3227
22. DeJonge, P. C., and Westerhoff, H. V. (1982) *Biochem. J.* **204,** 515–523
23. Wikström, M. (1984) *FEBS Lett.* **169,** 300–304
24. Scholes, T. A., and Hinkle, P. C. (1984) *Biochemistry* **23,** 3341–3345
25. Lemasters, J. J. (1984) *J. Biol. Chem.* **259,** 13123–13130
26. Hinkle, P. C. (1981) in *Chemiosmotic Proton Circuits in Biological Membranes* (Skulachev, V. P., and Hinkle, P. C., eds) pp. 49–58, Addison-Wesley Publishing Co., Reading, MA
27. Hatefi, Y., and Rieske, J. S. (1967) *Methods Enzymol* **10,** 235–239
28. Beyer, R. E. (1967) *Methods Enzymol.* **10,** 186–194
29. Smith, A. L. (1967) *Methods Enzymol.* **10,** 81–86
30. Wan, Y.-P., Williams, R. H., Folkers, K., Leung, K. H., and Racker, E. (1975) *Biochem. Biophys. Res. Commun.* **63,** 11–15
31. Albracht, S. P. J., Dooijewaard, G., Leeuwerik, F. J., and van Swol, B. (1977) *Biochim. Biophys. Acta* **459,** 300–317
32. Rich, P., and Bonner, W. D. (1978) in *Functions of Alternative Respiratory Oxidases* (Lloyd, D., Degn, H., and Hill, G. C., eds) pp. 61–68, Pergamon, New York
33. Azzi, A., Montecucco, C., and Richter, C. (1975) *Biochem. Biophys. Res. Commun.* **65,** 597–603
34. Takeshige, K., and Minakami, S. (1979) *Biochem. J.* **180,** 129–135
35. Ksenzenko, M., Konstantinov, A. A., Khomutov, G. B., Tikhonov, A. N., and Ruuge, E. K. (1983) *FEBS Lett.* **155,** 19–24
36. Turrens, J. F., and Boveris, A. (1980) *Biochem. J.* **191,** 421–427
37. Tyler, D. D., Butlow, R. A., Gonze, J., and Estabrook, R. W. (1965) *Biochem. Biophys. Res. Commun.* **19,** 551–557
38. Gutman, M., Kearney, E. B., Mayr, M., and Singer, T. P. (1971) *Physiol. Chem. Physics* **3,** 319–335
39. Case, G. D., Ohnishi, T., and Leigh, J. S. (1976) *Biochem. J.* **160,** 785–795
40. Ohnishi, T., and Salerno, J. C. (1982) in *Iron-Sulfur Proteins* (Spiro, T. G., ed) Vol. 4, pp. 285–327, John Wiley & Sons, New York
41. Gaudemer, Y., and Latruffe, N. (1975) *FEBS Lett.* **54,** 30–34
42. Spande, T. F., and Witkop, B. (1967) *Methods Enzymol.* **11,** 506–527
43. Heinrikson, R. L., and Kramer, K. J. (1974) in *Progr. Bioorg. Chem.* **3,** 141–250
44. Vik, S. B., and Hatefi, Y. (1984) *Biochem. Int.* **9,** 547–555
45. Beyer, R. E., Brink, T. W., Crankshaw, D. L., Kuner, J. M., and Pasternak, A. (1972) *Biochemistry* **11,** 961–969
46. Yagi, T. (1987) *Biochemistry* **26,** 2822–2828
47. Phillips, M. K., and Kell, D. B. (1982) *FEBS Lett.* **104,** 248–250
48. Chazotte, B., and Vanderkooi, G. (1981) *Biochim. Biophys. Acta* **636,** 153–161
49. Tyler, D. D. (1974) *Biochim. Biophys. Acta* **396,** 335–346
50. Gutman, M., and Silman, N. (1974) *FEBS Lett.* **47,** 241–243
51. Chance, B., and Hollunger, G. (1961) *J. Biol. Chem.* **236,** 1577–1584
52. Racker, E., and Kandrach, A. (1973) *J. Biol. Chem.* **248,** 5841–5847
53. Hinkle, P. C., Butlow, R. A., Racker, E., and Chance, B. (1967) *J. Biol. Chem.* **242,** 5169–5173
54. Cadenas, E., Boveris, A., Ragan, C. I., and Stoppani, A. O. M. (1977) *Arch. Biochem. Biophys.* **180,** 248–257
55. Kang, D., Narabayashi, H., Sata, T., and Takeshige, K. (1983) *J. Biochem. (Tokyo)* **94,** 1301–1306
56. Bruice, T. C. (1984) in *Flavins and Flavoproteins* (Bray, R. C., Engel, P. C., and Mayhew, S. G., eds) pp. 45–55, Walter de Gruyter, Berlin
57. Cadenas, E., and Boveris, A. (1980) *Biochem. J.* **188,** 31–37
58. Ksenzenko, M., Knostantinov, A. A., Khomutov, G. B., Tikhonov, A. N., and Ruuge, E. K. (1984) *FEBS Lett.* **175,** 105–108
59. Hatefi, Y., and Stempel, K. E. (1969) *J. Biol. Chem.* **244,** 2350–2357
60. Clark, W. M. (1960) *Oxidation-Reduction Potentials of Organic Systems,* Williams & Wilkins, Baltimore, MD
61. Chan, P. C., and Bielski, B. H. J. (1974) *J. Biol. Chem.* **249,** 1317–1319
62. Chan, P. C., and Bielski, B. H. J. (1980) *J. Biol. Chem.* **255,** 874–876
63. Suzuki, H., and King, T. E. (1983) *J. Biol. Chem.* **258,** 352–358
64. Dooijeward, G., and Slater, E. C. (1976) *Biochim. Biophys. Acta* **440,** 1–35
65. Wikström, M., Krab, K., and Saraste, M. (1981) *Annu. Rev. Biochem.* **50,** 623–655
66. Massey, V., and Hemmerich, P. (1980) *Biochem. Soc. Trans.* **8,** 246–257